Table 1 Clinical characteristics of all the patients of each genotype of T-138C

	Characteristic	CC (n = 17)	CT (n = 70)	TT (n = 47)	p value[a]
Basic	Age at the beginning of HD (years)	61 (44, 72)	57 (49, 69)	57 (50, 68)	0.90
	Age at the time of this study	62 (48, 74)	63 (53.8, 74)	60 (53, 70)	0.85
	Male % (n)	82.4 (14)	68.6 (48)	70.2 (33)	0.53
	Body mass index (kg/m^2)	21.6 (19.0, 24.2)	22.4 (20.4, 24.9)	22.6 (20.0, 23.9)	0.53
	HD duration (month)	26 (18, 39)	42 (23, 74)	41 (22, 77)	0.10
	Diabetes % (n)	23.5 (4)	47.1 (33)	40.4 (19)	0.20
Medications (po)	Statin % (n)	23.5 (4)	11.4 (8)	10.6 (5)	0.35
	Antihypertensives				
	Calcium channel blocker % (n)	13.3 (2)	30.0 (21)	36.2 (17)	0.17
	ACE inhibitor % (n)	0.0 (0)	1.4 (1)	2.1 (1)	0.82
	ARB % (n)	17.7 (3)	31.4 (22)	27.7 (13)	0.52
	Vitamin K % (n)	5.9 (1)	1.4 (1)	4.3 (2)	0.51
	Antiplatelet % (n)	29.4 (5)	37.1 (26)	31.9 (15)	0.76
	Warfarin % (n)	0.0 (0)	4.3 (3)	4.3 (2)	0.69
	Calcium carbonate % (n)	70.6 (12)	81.4 (57)	85.1 (40)	0.42
	Active vitamin D % (n)	82.4 (14)	60.0 (42)	57.5 (27)	0.17
	Sevelamar hydrochloride % (n)	17.7 (3)	27.1 (19)	23.4 (11)	0.70
	Cinacarcet % (n)	0.0 (0)	1.4 (1)	4.3 (2)	0.48
	Lanthanum carbonate % (n)	11.8 (2)	14.3 (10)	12.8 (6)	0.95
	Steroid % (n)	5.9 (1)	5.7 (4)	2.1 (1)	0.63
HD-related parameters	Kt/V	1.49 (1.41, 1.62)	1.46 (1.30, 1.67)	1.48 (1.33, 1.60)	0.80
	HD (hours)	4 (4, 4)	4 (4, 4)	4 (4, 4)	0.69
Laboratory data (blood)	Total protein (mg/dL)	6.3 (6.1, 6.5)	6.2 (5.9, 6.6)	6.2 (6.0, 6.6)	0.54
	Albumin (mg/dL)	3.6 (3.5, 3.9)	3.6 (3.4, 3.8)	3.7 (3.5, 3.8)	0.14
	Total cholesterol (mg/dL)	163 (136, 184)	154 (136, 180)	156 (139, 176)	0.97
	HDL cholesterol (mg/dL)	54 (40, 62)	42 (33, 51)	38 (32, 53)	0.03*
	LDL cholesterol (mg/dL)	67 (55, 104)	78 (67, 100)	78 (66, 97)	0.62
	Triglyceride (mg/dL)	123 (63, 156)	105 (70, 158)	119 (85, 223)	0.32
	Blood glucose (mg/dL)	128 (113, 151)	126 (102, 146)	125 (96, 151)	0.88
	HbA1c (%): only diabetic patients (n = 4:33:19)	5.7 (5.4, 8.3)	5.8 (5.5, 7.6)	6.2 (5.5, 6.7)	0.98
	GA (%): only diabetic patients (n = 4:33:19)	19.7 (17.2, 29.5)	19.5 (16.7, 23.6)	22.0 (20.3, 24.6)	0.12
	C-reactive protein (mg/dL)	0.1 (0.0, 0.2)	0.1 (0.0, 0.4)	0.1 (0.0, 0.2)	1.00
	Calcium (mg/dL)	9.0 (8.2, 9.5)	8.9 (8.6, 9.4)	9.1 (8.6, 9.7)	0.41
	Phosphate (mg/dL)	4.6 (3.8, 5.4)	4.9 (4.0, 5.6)	4.8 (4.2, 5.6)	0.46
	Calcium × phosphate	40.9 (32.0, 48.6)	43.4 (34.0, 49.6)	44.2 (36.9, 53.0)	0.30
	Intact-PTH (pg/mL)	75 (36, 105)	74 (39, 129)	63 (39, 145)	0.86
	Hemoglobin (g/dL)	11.2 (10.7, 11.7)	11.1 (10.5, 11.7)	10.9 (10.4, 11.8)	0.79
	Ferritin (ng/mL)	126 (94, 158)	132 (79, 192)	130 (55, 173)	0.64
	β2 microglobulin (mg/L)	23.9 (20.1, 26.0)	25.8 (22.0, 30.9)	25.8 (23.1, 30.6)	0.16
	Blood urea nitrogen (mg/dL)	64.8 (51.5, 81.9)	63.8 (56.5, 76.2)	69.1 (60.6, 80.0)	0.39
	Creatinine (mg/dL)	11.40 (9.33, 13.58)	11.73 (9.61, 13.39)	11.63 (10.22, 14.02)	0.70

Data are presented in % (n) for categorical variables, and as median (25th, 75th percentile) for continuous variables

We analyzed the MGP concentrations in the sera of 48 MHD patients (CC: n = 7, CT: n = 26, TT: n = 15) because of discontinuation of the kit from Biomedica. There were no significant differences in the serum MGP concentration among the genotypes (CC: 22.57 (21.41, 28.43), CT: 25.10 (21.23, 26.87), TT: 25.01 (23.07, 26.45), unit: nmol/L, p = 0.72)

ACE angiotensin-converting enzyme, *ARB* angiotensin receptor blocker, GA glycated albumin, *HD* hemodialysis, *HDL* high-density lipoprotein, *LDL* low-density lipoprotein *PTH* parathyroid hormone

* $p < 0.05$

[a] Chi-squared test was used for categorical variables, and Kruskal–Wallis tests were used for continuous variables

in arterial walls may be a central mechanism counteracting the progression of excessive VC. Furthermore, a recent study reported that gremlin, one of the bone morphogenetic protein (BMP) antagonists, binds to precursors of BMP and inhibits their function [29]. BMP is an osteoinductive factor expressed in atherosclerotic lesions and MGP is

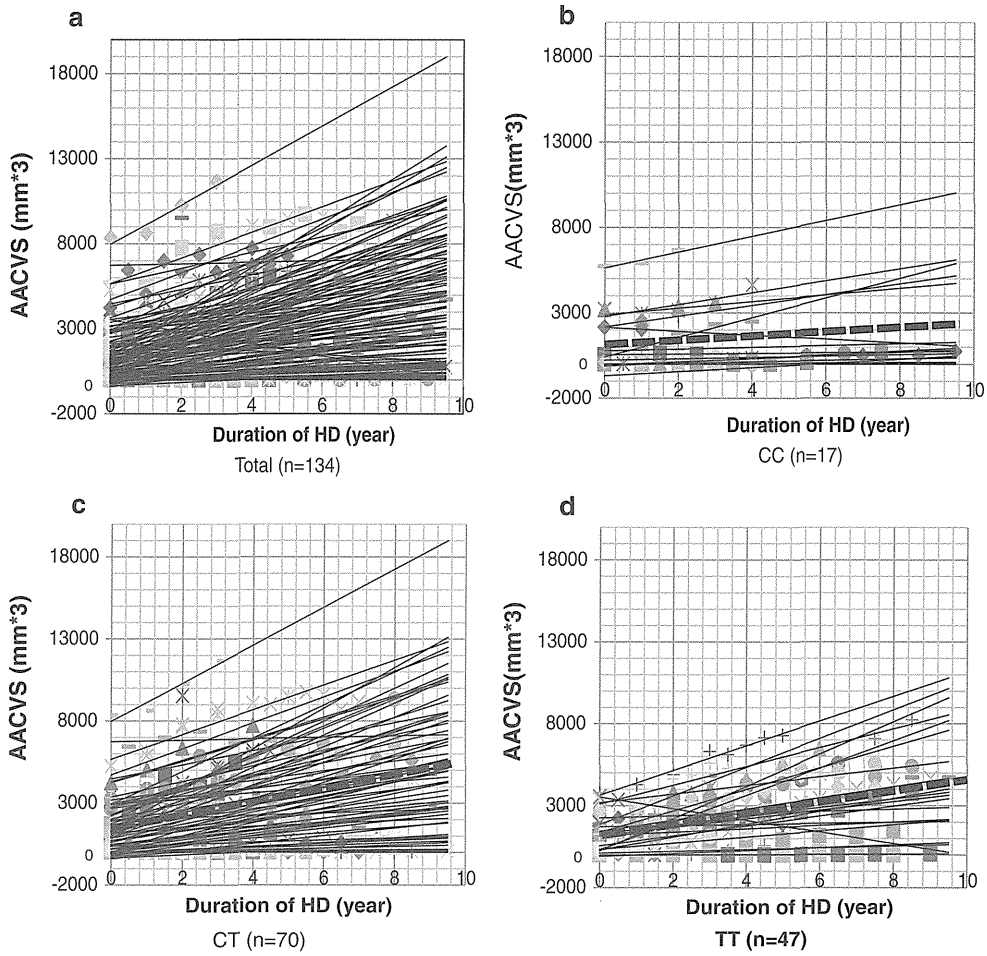

Fig. 4 Plots of the abdominal aortic calcium volume score (AACVS) as a linear function of each patients. **a** Plots of total patients (mean $R^2 = 0.87$). **b** Plots of only patients with the CC genotype of T-138C. **c** Plots of only patients with the CT genotype of T-138C. **d** Plots of only patients with the TT genotype of T-138C. The *dashed line* shows the mean scores for all patients in each genotype group

thought to be a BMP inhibitor. Therefore, the intracellular function to block BMP activation may be true of MGP and MGP may prevent arteries from calcification. Together with these findings, our study suggests that the CC genotype of T-138C may enhance the local activation of MGP independently of the serum MGP concentration, and may have the potential to inhibit VC in MHD patients.

We performed multiple regression analysis by the best subset regression method between the progression speed of VC and related parameters (Table 2), suggesting that the CC genotype of T-138C would function as a preventive factor for VC. Moreover, greater age at the beginning of MHD, high levels of Ca × P, low levels of HDL cholesterol, high levels of LDL cholesterol, and non-use of ARBs are all classic factors contributing to the progression of VC. With regard to gender, Yamada et al. [30] previously showed that the progression of AAC was negatively associated with the premenopausal status in women, which was considered to be due to female sex hormones. In our study, however, 34 of 39 (87.2 %) female participants were >50 years. Additionally, in our study, the CC genotype of T-138C was associated with higher concentrations of HDL cholesterol in the cross-sectional data (Table 1), and low levels of HDL cholesterol were significantly associated with progression of VC (Table 2). Yao et al. [31] previously reported in vitro that an increasing concentration of HDL cholesterol progressively enhanced expression of the activin-like kinase receptor 1 (ALK1) in human aortic endothelial cells, and that induction of ALK1 was associated with increased levels of MGP as determined by real-time PCR. This report supports our present data because high levels of HDL cholesterol may induce upregulation of focal MGP expression in the artery wall and subsequently halt the progression of VC. However, further investigations are needed to fully understand the mechanisms of regulation of HDL level in the CC genotype. Additionally, we tried taking the presence of diabetes, blood glucose and dialysis vintage (month) into the multiple regression analysis by the conventional model and the best subset regression method (stepwise method). These parameters were found not to influence the progression speed of VC in our analysis. Collectively, the most important finding in our study was that the MGP genotype was an invariable parameter related to the longitudinal VC progression.

There were several limitations to our study. The sample size of the study population was relatively small for a genetic association study. Therefore, further studies with a larger

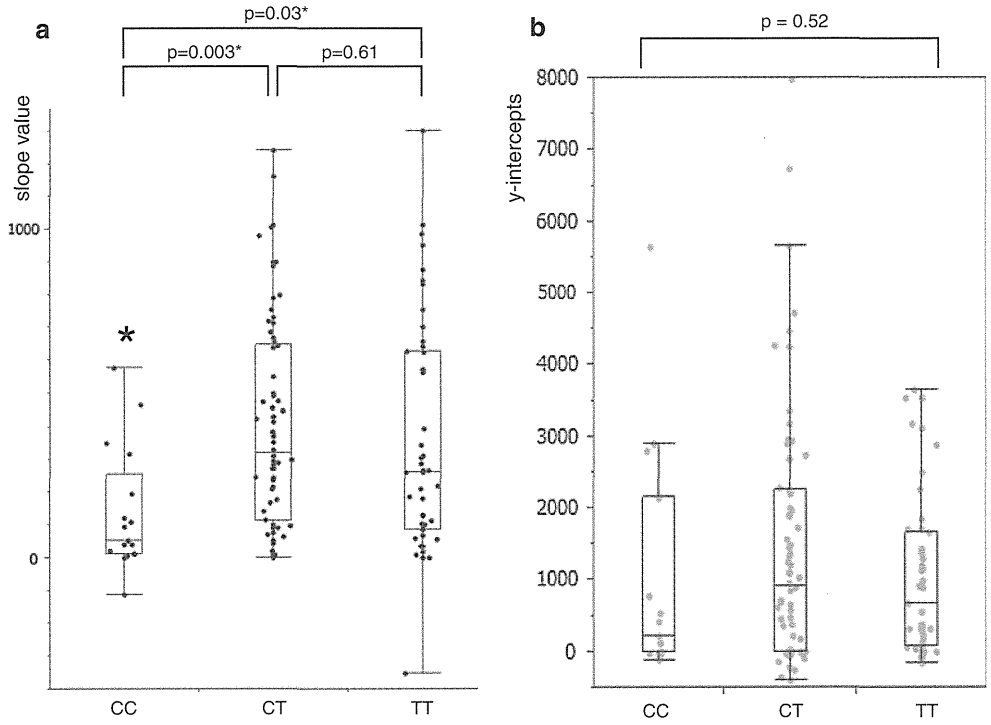

Fig. 5 The comparison of the progression speed of vascular calcification among the T-138C genotype. **a** The differences of the progression speed of the abdominal aortic calcium volume score (AACVS). **b** The comparison result of the vascular calcification (VC) at the beginning of HD (*y*-intercepts). Both were analyzed by Kruskal–Wallis test and Steel–Dwass test

Table 2 Multiple regression analysis between the progression speed of AACVS and related parameters

Covariate	Coefficient	95 % CI	Standardized β	*p* value
CT/TT genotype of T-138C	87.06	(19.04, 155.07)	0.25	0.01*
Age at the beginning of HD (years)	9.10	(5.14, 13,07)	0.38	<0.001*
Female sex	−73.30	(−127.38, −19.22)	−0.20	0.008*
Ca × P	9.15	(4.61, 13.70)	0.33	<0.001*
HDL cholesterol (mg/dL)	−3.44	(−6.60, −0.28)	−0.16	0.03*
LDL cholesterol (mg/dL)	3.09	(1.10, 5.07)	0.23	0.003*
Ferritin (ng/mL)	−0.65	(−1.13, −0.16)	−0.20	0.01*
ARBs	−63.70	(−117.61, −9.78)	−0.18	0.02*

$n = 134$, $R^2 = 0.34$, $F = 7.1936$, $p < 0.001$, Durbin–Watson ratio 1.9365483

ARBs angiotensin receptor blockers, *Ca* × *P* calcium × phosphate, *HD* hemodialysis, *HDL* high-density lipoprotein, *LDL* low-density lipoprotein

* $p < 0.05$

number of subjects in different groups with different characteristics are needed. We need to continue this study prospectively in order to investigate relationships to cardiovascular events and long-term mortality. In addition, large-scale follow-up studies with high-risk CKD patients would enhance and vary the information about the genetic background.

Conclusions

This study emphasizes that MGP T-138C polymorphism is closely linked to the progression speed of VC in MHD patients. VC is very common in MHD patients and is a strong predictor of cardiovascular disease and all-cause mortality. In particular, accelerated progressive VC strongly deteriorates the prognosis of MHD patients. We propose here that the genotype of the *MGP* gene might be a genomic biomarker that is predictive of VC progression. Furthermore, this inalterable biomarker may be helpful for disease detection and classification, treatment response prediction, treatment efficacy, and prognosis.

Acknowledgments The authors thank A. Sakurai, T. Sasaki, and S. Hayashi for their technical support. This study was supported in part

by a Grant-in-Aid for Diabetic Nephropathy, Research from the Ministry of Health, Labour and Welfare of Japan and a grant from The Kidney Foundation, Japan (JKFB10-28 and JKF10-2).

Conflict of interest The authors have declared that no conflict of interest exists.

References

1. Raggi P, Boulay A, Chasan-Taber S, Amin N, Dillon M, Burke SK, et al. Cardiac calcification in adult hemodialysis patients. A link between end-stage renal disease and cardiovascular disease? J Am Coll Cardiol. 2002;39:695–701.
2. Goodman WG, Goldin J, Kuizon BD, Yoon C, Gales B, Sider D, et al. Coronary-artery calcification in young adults with end-stage renal disease who are undergoing dialysis. N Engl J Med. 2000;342:1478–83.
3. Block GA, Spiegel DM, Ehrlich J, Mehta R, Lindbergh J, Dreisbach A, et al. Effects of sevelamer and calcium on coronary artery calcification in patients new to hemodialysis. Kidney Int. 2005;68:1815–24.
4. Blacher J, Guerin AP, Pannier B, Marchais SJ, London GM. Arterial calcifications, arterial stiffness, and cardiovascular risk in end-stage renal disease. Hypertension. 2001;38:938–42.
5. London GM, Guérin AP, Marchais SJ, Métivier F, Pannier B, Adda H. Arterial media calcification in end-stage renal disease: impact on all-cause and cardiovascular mortality. Nephrol Dial Transplant. 2003;18:1731–40.
6. Maréchal C, Schlieper G, Nguyen P, Krüger T, Coche E, Robert A, et al. Serum fetuin-A levels are associated with vascular calcifications and predict cardiovascular events in renal transplant recipients. Clin J Am Soc Nephrol. 2011;6:974–85.
7. Price PA, Otsuka AS, Poser JW, Kristaponis J, Raman N. Characterization of a gamma-carboxyglutamic acid-containing protein from bone. Proc Natl Acad Sci USA. 1976;73:1447–51.
8. Covic A, Kanbay M, Voroneanu L, Turgut F, Serban DN, Serban IL, et al. Vascular calcification in chronic kidney disease. Clin Sci (Lond). 2010;119:111–21.
9. Luo G, Ducy P, McKee MD, Pinero GJ, Loyer E, Behringer RR, et al. Spontaneous calcification of arteries and cartilage in mice lacking matrix GLA protein. Nature. 1997;386:78–81.
10. Moe SM, Chen NX. Pathophysiology of vascular calcification in chronic kidney disease. Circ Res. 2004;95:560–7.
11. Braam LA, Dissel P, Gijsbers BL, Spronk HM, Hamulyák K, Soute BA, et al. Assay for human matrix gla protein in serum: potential applications in the cardiovascular field. Arterioscler Thromb Vasc Biol. 2000;20:1257–61.
12. Herrmann SM, Whatling C, Brand E, Nicaud V, Gariepy J, Simon A, et al. Polymorphisms of the human matrix gla protein (MGP) gene, vascular calcification, and myocardial infarction. Arterioscler Thromb Vasc Biol. 2000;20:2386–93.
13. Farzaneh-Far A, Davies JD, Braam LA, Spronk HM, Proudfoot D, Chan SW, et al. A polymorphism of the human matrix gamma-carboxyglutamic acid protein promoter alters binding of an activating protein-1 complex and is associated with altered transcription and serum levels. J Biol Chem. 2001;276:32466–73.
14. Brancaccio D, Biondi ML, Gallieni M, Turri O, Galassi A, Cecchini F, et al. Matrix GLA protein gene polymorphisms: clinical correlates and cardiovascular mortality in chronic kidney disease patients. Am J Nephrol. 2005;25:548–52.
15. Crosier MD, Booth SL, Peter I, Dawson-Hughes B, Price PA, O'Donnell CJ, et al. Matrix Gla protein polymorphisms are associated with coronary artery calcification in men. J Nutr Sci Vitaminol (Tokyo). 2009;55:59–65.
16. Schurgers LJ, Teunissen KJ, Knapen MH, Geusens P, van der Heijde D, Kwaijtaal M, et al. Characteristics and performance of an immunosorbent assay for human matrix Gla-protein. Clin Chim Acta. 2005;351:131–8.
17. Callister TQ, Cooil B, Raya SP, Lippolis NJ, Russo DJ, Raggi P. Coronary artery disease: improved reproducibility of calcium scoring with an electron-beam CT volumetric method. Radiology. 1998;208:807–14.
18. Floege J, Raggi P, Block GA, Torres PU, Csiky B, Naso A, et al. Study design and subject baseline characteristics in the ADVANCE Study: effects of cinacalcet on vascular calcification in haemodialysis patients. Nephrol Dial Transplant. 2010;25:1916–23.
19. Raggi P, Callister TQ, Shaw LJ. Progression of coronary artery calcium and risk of first myocardial infarction in patients receiving cholesterol-lowering therapy. Arterioscler Thromb Vasc Biol. 2004;24:1272–7.
20. Block GA, Raggi P, Bellasi A, Kooienga L, Spiegel DM. Mortality effect of coronary calcification and phosphate binder choice in incident hemodialysis patients. Kidney Int. 2007;71:438–41.
21. Kauppila LI, Polak JF, Cupples LA, Hannan MT, Kiel DP, Wilson PW. New indices to classify location, severity and progression of calcific lesions in the abdominal aorta: a 25-year follow-up study. Atherosclerosis. 1997;132:245–50.
22. Wilson PW, Kauppila LI, O'Donnell CJ, Kiel DP, Hannan M, Polak JM, et al. Abdominal aortic calcific deposits are an important predictor of vascular morbidity and mortality. Circulation. 2001;103:1529–34.
23. Walsh CR, Cupples LA, Levy D, Kiel DP, Hannan M, Wilson PW, et al. Abdominal aortic calcific deposits are associated with increased risk for congestive heart failure: the Framingham Heart Study. Am Heart J. 2002;144:733–9.
24. Bellasi A, Ferramosca E, Muntner P, Ratti C, Wildman RP, Block GA, et al. Correlation of simple imaging tests and coronary artery calcium measured by computed tomography in hemodialysis patients. Kidney Int. 2006;70:1623–8.
25. Okuno S, Ishimura E, Kitatani K, Fujino Y, Kohno K, Maeno Y, et al. Presence of abdominal aortic calcification is significantly associated with all-cause and cardiovascular mortality in maintenance hemodialysis patients. Am J Kidney Dis. 2007;49:417–25.
26. Karsli Ceppioglu S, Yurdun T, Canbakan M. Assessment of matrix gla protein, klotho gene polymorphisms, and oxidative stress in chronic kidney disease. Ren Fail. 2011;33:866–74.
27. Shanahan CM, Cary NR, Metcalfe JC, Weissberg PL. High expression of genes for calcification-regulating proteins in human atherosclerotic plaques. J Clin Invest. 1994;93:2393–402.
28. Dhore CR, Cleutjens JP, Lutgens E, Cleutjens KB, Geusens PP, Kitslaar PJ, et al. Differential expression of bone matrix regulatory proteins in human atherosclerotic plaques. Arterioscler Thromb Vasc Biol. 2001;21:1998–2003.
29. Sun J, Zhuang FF, Mullersman JE, Chen H, Robertson EJ, Warburton D, et al. BMP4 activation and secretion are negatively regulated by an intracellular gremlin-BMP4 interaction. J Biol Chem. 2006;281:29349–56.
30. Yamada K, Fujimoto S, Nishiura R, Komatsu H, Tatsumoto M, Sato Y, et al. Risk factors of the progression of abdominal aortic calcification in patients on chronic haemodialysis. Nephrol Dial Transplant. 2007;22:2032–7.
31. Yao Y, Shao ES, Jumabay M, Shahbazian A, Ji S, Boström KI. High-density lipoproteins affect endothelial BMP-signaling by modulating expression of the activin-like kinase receptor 1 and 2. Arterioscler Thromb Vasc Biol. 2008;28:2266–74.

Anal Bioanal Chem (2012) 404:3101–3109
DOI 10.1007/s00216-012-6412-x

ORIGINAL PAPER

Metabolic profiling reveals new serum biomarkers for differentiating diabetic nephropathy

Akiyoshi Hirayama · Eitaro Nakashima · Masahiro Sugimoto · Shin-ichi Akiyama · Waichi Sato · Shoichi Maruyama · Seiichi Matsuo · Masaru Tomita · Yukio Yuzawa · Tomoyoshi Soga

Received: 2 July 2012 / Revised: 4 September 2012 / Accepted: 5 September 2012 / Published online: 29 September 2012

Abstract Capillary electrophoresis coupled with time-of-flight mass spectrometry was used to explore new serum biomarkers with high sensitivity and specificity for diabetic nephropathy (DN) diagnosis, through comprehensive analysis of serum metabolites with 78 diabetic patients. Multivariate analyses were used for identification of marker candidates and development of discriminative models. Of the 289 profiled metabolites, orthogonal partial least-squares discriminant analysis identified 19 metabolites that could distinguish between DN with macroalbuminuria and diabetic patients without albuminuria. These identified metabolites included creatinine, aspartic acid, γ-butyrobetaine, citrulline, symmetric dimethylarginine (SDMA), kynurenine, azelaic acid, and galactaric acid. Significant correlations between all these metabolites and urinary albumin-to-creatinine ratios ($p<0.009$, Spearman's rank test) were observed. When five metabolites (including γ-butyrobetaine, SDMA, azelaic acid and two unknowns) were selected from 19 metabolites and applied for multiple logistic regression model, AUC value for diagnosing DN was 0.927 using the whole dataset, and 0.880 in a cross-validation test. In addition, when four known metabolites (aspartic acid, SDMA, azelaic acid and galactaric acid) were applied, the resulting AUC was still high at 0.844 with the whole dataset and 0.792 with cross-validation. Combination of serum metabolomics with multivariate analyses enabled accurate discrimination of DN patients. The results suggest that capillary electrophoresis-mass spectrometry based metabolome analysis could be used for DN diagnosis.

Keywords Diabetic nephropathy · Capillary electrophoresis-mass spectrometry · Metabolome · Biomarker · Multiple logistic regression · Orthogonal partial least-squares discriminant analysis

A. Hirayama · M. Sugimoto · M. Tomita · T. Soga (✉)
Institute for Advanced Biosciences, Keio University,
246-2 Mizukami, Kakuganji,
Tsuruoka, Yamagata 997-0052, Japan
e-mail: soga@sfc.keio.ac.jp

E. Nakashima
Japan Labour Health and Welfare Organization Chubu Rosai Hospital,
1-10-6 Koumei-cho, Minato-ku,
Nagoya, Aichi 455-8530, Japan

E. Nakashima
Department of Endocrinology and Diabetes, Nagoya University Graduate School of Medicine,
65 Tsurumai-cho, Showa-ku,
Nagoya, Aichi 466-8550, Japan

M. Sugimoto
Medical Innovation Center, Kyoto University Graduate School of Medicine,
Yoshida Konoe, Sakyo-ku,
Kyoto 606-8501, Japan

S.-i. Akiyama · W. Sato · S. Maruyama · S. Matsuo · Y. Yuzawa
Department of Nephrology of Internal Medicine, Nagoya University Graduate School of Medicine,
65 Tsurumai-cho, Showa-ku,
Nagoya, Aichi 466-8550, Japan

Introduction

Diabetic nephropathy (DN) is one of the major complications of diabetes mellitus (DM) and has become the most prevalent cause of end-stage renal disease worldwide [1]. DN is also one of the most significant long-term diseases in terms of morbidity and mortality for individuals with diabetes [2]. Recent

studies have shown that several interventions can slow the progression of DN, and their impact is greater if they are started at an early stage of the development of nephropathy [3]. Although renal biopsy is the most accurate diagnostic method for DN, routine renal biopsies are not acceptable in current clinical practice because of their invasiveness. Microalbuminuria is an alternative, non-invasive marker that can be used for DN risk assessment, and the urinary albumin-to-creatinine ratio (UACR) on first-void urine sample is recommended for DN screening. However, large prospective studies have revealed poor accuracy of this marker, even though urine samples are collected two or three times a day to normalize day-to-day variation [4]. Therefore, identifying reliable and versatile biomarkers for risk assessment of DN is important.

Mass spectrometry-based urinary proteomics is used for biomarker discoveries of DN. Dihazi et al. used surface-enhanced laser desorption/ionization time-of-flight mass spectrometry to identify three urinary proteins that differentiated patients with DN from patients with type 2 DM without nephropathy, patients with type 2 DM with micro- or macroalbuminuria, patients with proteinuria caused by non-diabetic renal disease, and healthy controls [5]. Mischak et al. profiled urinary polypeptides using capillary electrophoresis-mass spectrometry (CE-MS) and found that the MS patterns could be used to differentiate type 2 DM from healthy controls [6]. However, urinary protein markers sometimes show a wider variation than blood samples. Thus, it is necessary to discover biomarkers with small diurnal variations.

Metabolomics is the comprehensive analysis of low weight molecules in a sample, and has become a powerful tool in the biomarker discovery field. Nuclear magnetic resonance [7], gas chromatography-mass spectrometry [8], liquid chromatography-mass spectrometry (LC-MS; [9]), and CE-MS [10–12] are currently used for metabolomics. Targeted profiling, that is, detection of only a few sets of metabolites, has been used to discover biomarkers for DN. Xia et al. analyzed six intermediate metabolites of the purine degradation pathway in plasma from patients with non-DN and DN using LC with or without MS [13]. They found that adenosine, inosine, uric acid, and xanthine were useful biomarkers for monitoring DM progression. Jiang et al. used LC-tandem mass spectrometry to simultaneously quantify eight aminothiols in the homocysteine metabolic cycle in plasma and found two sulfur-containing metabolites, *S*-adenosylmethionine and *S*-adenosylhomocysteine, as potential biomarkers for DM and DN [14].

Compared to targeted profiling, comprehensive metabolome analysis of all metabolites in the given sample is a more powerful technique. Zhang et al. used non-targeted LC-MS to detect potential biomarker candidates of DN and type 2 DM, and observed significant differences in the serum levels of leucine, dihydrosphingosine, and phytosphingosine [15]. However, there are few published comprehensive metabolome profiles of DN.

Recently, we developed a non-targeted CE-MS-based metabolome profiling technique [11, 16] and applied it to biomarker discovery for acetaminophen-induced hepatotoxicity in mice [11] and several types of cancer-specific profiles in human saliva [12]. In the present study, we used CE-MS to identify serum metabolite biomarkers for DN diagnosis. Furthermore, classification models incorporating multiple biomarkers were constructed for discriminating DN from non-DN.

Materials and methods

Sample collection and metabolite extraction

All experiments were conducted in accordance with study protocol approved by the Institutional Ethics Committee of Chubu Rosai Hospital. Informed consent was obtained from all patients according to the Declaration of Helsinki as revised in 2000. Serum samples from 78 type 2 DM patients were collected and classified into the following three groups: DM group without nephropathy and albuminuria (non-DN, UACR<30 mg/g, n=20), early DN group with microalbuminuria (micro-DN, 30<UACR<300 mg/g, n=32), and overt DN group with macroalbuminuria (macro-DN, UACR>300 mg/g, n=26). All serum samples were stored at −80 °C.

To extract metabolites, the frozen sera samples were thawed and 100 μl aliquots were put into 900 μl of methanol that contained internal standards (20 μmol/l each of methionine sulfone and camphor 10-sulfonic acid). The internal standards were used to normalize the extraction efficiency of metabolites during sample preparation for both cationic (methionine sulfone) and anionic (camphor 10-sulfonic acid) metabolite analysis. The solutions were mixed well and then 400 μl of Milli-Q water and 1 ml of chloroform were added, followed by centrifugation at 4,600×g for 5 min at 4 °C. The aqueous layer was transferred to a 5-kDa cutoff centrifugal filter tube (Millipore, Billerica, MA, USA) to remove large molecules. The filtrate was centrifugally concentrated at 35 °C and reconstituted with 50 μl of Milli-Q water that contained reference compounds (200 μmol/l each of 3-aminopyrrolidine and trimesic acid) immediately before CE-TOFMS analysis. These reference compounds were added to eliminate the variation in migration time of individual peaks in electropherogram among multiple datasets.

Reagents

Methionine sulfone (internal standard) was purchased from Alfa Aesar (Ward Hill, MA), and hexakis-(2,2-difluoroethoxy)-phosphazene (Hexakis) from SynQuest

Laboratories (Alachua, FL). All other reagents were obtained from Sigma-Aldrich (St. Louis, MO) or Wako Pure Chemicals Industries Ltd. (Osaka, Japan). All chemicals used were of analytical or reagent grade. Water was purified with a Milli-Q purification system (Millipore, Billerica, MA).

Instruments

All CE-electrospray ionization (ESI)-TOFMS experiments were performed using an Agilent CE capillary electrophoresis system (Agilent Technologies, Waldbronn, Germany), an Agilent G3250AA LC/MSD TOF system (Agilent Technologies, Palo Alto, CA, USA), an Agilent 1100 series isocratic HPLC pump, a G1603A Agilent CE-MS adapter kit, and a G1607A Agilent CE-ESI-MS sprayer kit. The CE-MS adapter kit included a capillary cassette, which facilitated thermostating of the capillary, and the CE-ESI-MS sprayer kit, which simplified coupling of the CE system with the MS system, was equipped with an electrospray source. For system control and data acquisition, G2201AA Agilent Chemstation software was used for CE, and Agilent TOF (Analyst QS) software was used for TOFMS. The original Agilent SST316Ti stainless steel (Fe/Cr/Ni/Mo/Ti; 68:18:11:2:1) ESI needle was replaced with a platinum needle for anion analysis [17]. The resolution of the TOFMS instrument used in this study is higher than 3,000 at *m/z* 100 with high mass accuracy (<3 ppm).

CE-TOFMS analysis of cationic metabolites

CE-TOFMS analysis of cationic metabolites was performed as described previously [10]. Cationic metabolites were separated in a fused-silica capillary (50 μm i.d.×100 cm total length) filled with 1 mol/l formic acid as the reference electrolyte. The sample solution was injected at 5 kPa for 3 s (approximately 3 nl), and a positive voltage of 30 kV was applied. The capillary and sample trays were maintained at 20 °C and <5 °C, respectively. The sheath liquid was methanol/water (50 %*v*/*v*) containing 0.1 μmol/l Hexakis and was delivered at 10 μl/min. ESI-TOFMS was operated in positive ion mode. The capillary voltage was set at 4 kV, and the nitrogen gas (heater temperature 300 °C) flow rate was set at 10 l/min. In TOFMS, the fragmenter voltage, skimmer voltage, and octapole radio frequency voltage were set at 75, 50, and 125 V, respectively. An automatic recalibration function was performed using the following masses of two reference standards: [^{13}C isotopic ion of the protonated methanol dimer $(2MeOH + H)]^+$, *m/z* 66.06306; and [protonated Hexakis $(M + H)]^+$, *m/z* 622.02896. Mass spectra were acquired at a rate of 1.5 cycles per second from *m/z* 50 to 1000.

CE-TOFMS analysis of anionic metabolites

The CE-TOFMS analysis of anionic metabolites was performed as described previously [17]. Anionic metabolites were separated in a commercially available COSMO(+) capillary, which was chemically coated with a cationic polymer. Ammonium acetate solution (50 mmol/l, pH 8.5) was used as the electrolyte for CE separation. The sample solution was injected at 5 kPa for 30 s (approximately 30 nl) and a voltage of −30 kV was applied. Ammonium acetate (5 mmol/l) in methanol/water (50 %*v*/*v*) containing 0.1 μmol/l Hexakis was delivered as the sheath liquid at 10 μl/min. ESI-TOFMS was operated in negative ion mode. The capillary voltage was set at 3.5 kV. In TOFMS, the fragmenter voltage, skimmer voltage, and octapole radio frequency voltage were set at 100, 50, and 200 V, respectively. An automatic recalibration function was performed using the following masses of two reference standards: [^{13}C isotopic ion of deprotonated acetic acid dimer $(2CH_3COOH-H)]^-$, *m/z* 120.03834; and [Hexakis + deprotonated acetic acid $(M + CH_3COOH-H)]^-$, *m/z* 680.03554. Mass spectra were acquired at a rate of 1.5 cycles per second from *m/z* 50 to 1,000.

Data processing

The raw data were processed using our proprietary software (MasterHands) [10, 12]. The overall data processing flow consisted of noise filtering, baseline correction, peak detection, and integration of the peak areas from 0.02 *m/z*-wide sections of the electropherograms. Subsequently, the accurate *m/z* of each peak was calculated by Gaussian curve fitting in the *m/z* domain, and the migration times were normalized to match the detected peaks among the multiple datasets. The peaks were identified by matching *m/z* values and normalized migration times of corresponding authentic standard compounds. Processed peak lists were exported for further statistical analysis.

Statistical analysis

The relative ratio of the detected peak area to that of the internal standard was used to eliminate systematic bias derived from injection volume variance and MS sensitivity. Data were analyzed with GraphPad Prism 5.0 (GraphPad Software, Inc., San Diego, CA, USA) for statistical tests. The Kruskal–Wallis test and Dunn's post test were used to assess the statistical significance of differences among non-DN, micro-DN and macro-DN samples. The Spearman's rank correlation test was used to calculate correlations among UACR, eGFR, and the relative ratios of peak areas of the metabolites. Multiple logistic regression (MLR) models were developed to discriminate non-DN and DN cohorts. Biomarker metabolites for these models were selected in

two procedures. First, normalized data were subjected to orthogonal partial least-squares discriminant analysis (OPLS-DA) using SIMCA-P + software (Version 12.0, Umetrics, Umeå, Sweden), and a model was built and used to identify marker metabolites that accounted for differentiation of non-DN and macro-DN cohorts. Next, a stepwise variable selection method (forward and backward selection) was conducted with a threshold of $p<0.25$ for adding and eliminating features using JMP 8.0 (SAS Institute Inc., Cary, NC, USA). The generalization ability of the developed MLR model was evaluated using cross-validation methods. Tenfold cross-validation was conducted 20 times with different random seeds using WEKA (ver. 3.6.1, The University of Waikato, Hamilton, New Zealand) to split the datasets into training and validation data [18]. Bootstrap analysis was also conducted to estimate the optimistic bias in the given datasets. Two hundred replicates, including the same number of patients, were computationally generated with a random selection of individuals, this permitted redundant selection, and MLR models were developed and cross-validation tests were conducted on each generated dataset.

Results

Metabolome analysis of serum samples obtained from non-DN and DN patients

Serum metabolome profiles of 78 patients in three successive stages of DN were collected using a single standard protocol [non-DN (n=20), micro-DN (n=32) and macro-DN (n=26)] and analyzed. Age distribution, gender and other clinical characteristics are listed in Table 1. The ages in the micro-DN and macro-DN groups were slightly higher than in the non-DN group (p=0.0226). The macro-DN group had significantly higher creatinine contents and lower estimated glomerular filtration rates (eGFR) than the other groups ($p<0.0001$), while no significant difference was seen between the non-DN and micro-DN groups. The macro-DN group also showed significantly higher triglycerides and systolic blood pressure (SBP) compared with the non-DN group (p=0.0172 and 0.0083, respectively). The other clinical parameters showed no significant difference among all groups ($p>0.05$).

On average, 4400 peaks were detected from each serum sample with CE-TOFMS. After eliminating redundant peaks, such as noise, fragments and adduct ions, 289 metabolites remained. Using this dataset, we firstly performed principal component analysis (PCA), but the resultant score plots of the PCA showed no unequivocal stage-specific clusters (data not shown). Next, OPLS-DA was performed to discriminate between DN patients (micro-DN and macro-DN) and non-DN patients based on the profiled metabolites. The OPLS-DA model demonstrated satisfactory separation between non-DN and micro-DN patients (Fig. 1a) using one predictive component and one orthogonal component (R^2X_{cum}=0.21, R^2Y_{cum}=0.676, ${Q_{cum}}^2$=0.179), and clear separation between non-DN and macro-DN patients (Fig. 1b) using one predictive component and three orthogonal components (R^2X_{cum}=0.353, R^2Y_{cum}=0.946, ${Q_{cum}}^2$=0.599). These results indicate that serum metabolome profile can be used to distinguish DN patients from non-DN patients.

The resultant S plot of the developed OPLS-DA model between non-DN and macro-DN patients identified 19 metabolites (Table 2) that were highly correlated in the separation of the groups ($|p(corr)|>0.5$). Of these, we were able to assign metabolite identities to eight metabolites by matching their m/z values and migration times with those of standard reagents. These metabolites were creatinine, aspartic acid, γ-butyrobetaine, citrulline, symmetric dimethylarginine (SDMA), kynurenine, azelaic acid, and galactaric acid. The composition formulae of the other metabolites were calculated based on their isotope distribution patterns as follows: $C_5H_8N_2O_2$ [metabolite ID (MID) 17], $C_9H_{17}NO$ (MID 51), $C_9H_{19}NO$ (MID 52), $C_2H_4N_2O_3$ (MID 158), and $C_6H_6N_4O$ (MID 202). Only the m/z values of the other metabolites are listed in Table 2 because of insufficient isotope peak size. The AUC values of MID 202 (0.765, 95 % CI); 0.649–0.880, $p=4.47\times10^{-4}$) gave the best discriminating ability among these markers (Table 3).

Correlation between biomarker candidates and clinical parameters

Correlation analysis between these 19 serum biomarker candidates and currently available clinical parameters showed all candidate metabolites were significantly correlated with UACR ($p<0.009$) (Table 4). The correlation coefficients for creatinine (r=0.5701), aspartic acid (r=0.4993), γ-butyrobetaine (r=0.4942), citrulline (r=0.4300), SDMA (r=0.4820), kynurenine (r=0.5351), MID 17 (r=0.4968), MID 97 (r=0.5223), MID 152 (r=0.5336), MID 158 (r=0.4980), and MID 202 (r=0.6352) were positively correlated with UACR. Those of azelaic acid (r=–0.5210), galactaric acid (r=–0.4596), MID 51 (r=–0.4728), MID 52 (r=–0.4871), MID 96 (r=–0.3085), MID 114 (r=–0.3638), MID 127 (r=–0.2961), and MID 134 (r=–0.3669) were negatively correlated. Furthermore, 15 of 19 metabolites were significantly correlated with eGFR ($p<0.035$). The correlation coefficients of creatinine (r=–0.8832), aspartic acid (r=–0.3912), γ-butyrobetaine (r=–0.6492), citrulline (r=–0.6531), SDMA (r=–0.7111), kynurenine (r=–0.5627), MID 17 (r=–0.5808), MID 97 (r=–0.7651), MID 152 (r=–0.7687), MID 158 (r=–0.6302), and MID

Table 1 Clinical characteristics of diabetic nephropathy patients

	Non-DN	Micro-DN	Macro-DN	*p* value
Number	20	32	26	
Male/Female	9/11	22/10	17/9	
Age (years)	57.5±12.9	66.6±9.2[a]	67.3±8.7[a]	0.0226
BMI (kg/m^2)	26.9±5.0	24.6±3.4 (1)	24.8±3.0	0.3074
HbA_{1c} (%)	6.8±1.0	7.2±1.1	6.8±0.7	0.3931
UACR (mg/g)	12.1±6.7	103.9±77.8[a]	1055.3±741.3[a, b]	<0.0001
Creatinine (enzymatic, mg/dL)	0.71±0.18	0.84±0.28	1.39±0.66[a,b]	<0.0001
Triglycerides (mg/dL)	134.6±131.5	133.5±55.2	179.7±110.3[a] (3)	0.0172
Cholesterol (mg/dL)	190.4±53.5 (2)	198.5±25.7 (2)	218.0±41.9 (1)	0.0838
HDL cholesterol (mg/dL)	56.3±18.9	50.9±14.6	52.9±21.1 (1)	0.5011
LDL cholesterol (mg/dL)	120.4±31.7	120.5±26.2 (1)	125.8±34.1 (1)	0.8421
Systolic BP (mmHg)	132±21	143±23	152±22[a]	0.0083
Diastolic BP (mmHg)	74±13	79±14	81±10	0.0711
eGFR (mL/min/1.73 m^2)	81.9±24.0	70.5±21.9	47.2±25.6[a,b]	<0.0001
Medication (number)				
Diabetic drug	17	27	25	
Hypolipidemic drug	10	16	14	
Antihypertensive drug	10	19	22	

The number in parentheses indicates the number of patients for which clinical values were missing. The *p* values were calculated using the data from the patients without missing values. Data are means±SD

[a]Significantly different compared to non-DN group

[b]Significantly different compared to micro-DN group

202 (r=–0.7455) showed negative correlation with eGFR. This indicates that they were positively associated with renal dysfunction. By contrast, those of azelaic acid (r=0.3739), galactaric acid (r=0.4152), MID 51 (r=0.2204), and MID 134 (r=0.2397) showed positive correlation with eGFR.

MLR model development

For the discrimination of DN (micro-DN and macro-DN) from non-DN patients, we developed a MLR model. Of the 19 biomarker candidates, γ-butyrobetaine, SDMA, azelaic acid, MID 114, and MID 127 were selected by stepwise feature selection as MLR variables. The developed model yielded high AUC values (0.927, 95 % CI, 0.870–0.983, p< 0.0001, Fig. 2a). The model also yielded high AUC values (±SD; 0.880±8.62×10^{-3}) in the cross-validation test. In a bootstrap test, the AUC values were 0.946±0.0262 and 0.895±0.0364 for training and cross-validation, respectively. To evaluate only the eight identified metabolites, we independently developed a MLR model. Stepwise feature selection selected aspartic acid, SDMA, azelaic acid, and galactaric acid as MLR variables. This MLR model also yielded high AUC values (0.844, 95 % CI, 0.754–0.934, p<0.0001, Fig. 2b), although it performed slightly worse than the model with all metabolites, including unknown peaks. This model also yielded high AUC values (±SD;

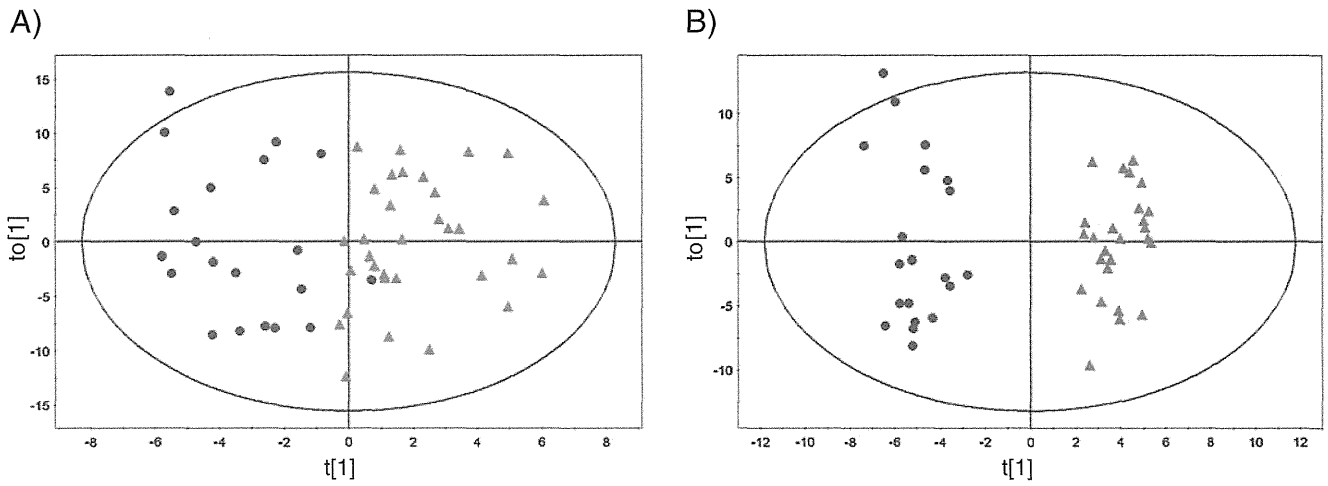

Fig. 1 OPLS-DA based on comprehensive metabolites data from (**A**) non-DN (*blue dots*) and micro-DN (*pink triangles*) samples and (**B**) non-DN (*blue dots*) and macro-DN (*red triangles*) samples. The *ellipse* in each figure indicates the Hotelling T2 (0.95) range for this model

Table 2 The 19 serum biomarker candidates that statistically differentiated the different DN stages

MID	Mode[a]	*m/z*	Non-DN	Micro-DN	Macro-DN	*p* value	Formula	Metabolite
11	C	114.067	0.501±0.153	0.612±0.209	1.052±0.506	<0.0001	$C_4H_7N_3O$	Creatinine
17	C	129.067	0.046±0.035	0.065±0.049	0.125±0.079	<0.0001	$C_5H_8N_2O_2$	
29	C	134.046	0.126±0.025	0.141±0.041	0.170±0.036	<0.0001	$C_4H_7NO_4$	Aspartic acid
39	C	146.118	0028±0.007	0.032±0.008	0.039±0.010	<0.0001	$C_7H_{16}NO_2$	γ-Butyrobetaine
51	C	156.139	0.006±0.005	0.005±0.004	0.001±0.003	0.0005	$C_9H_{17}NO$	
52	C	158.154	0.063±0.020	0.055±0.022	0.040±0.012	0.0007	$C_9H_{19}NO$	
69	C	176.104	0.194±0.053	0.199±0.060	0.275±0.081	0.0005	$C_6H_{13}N_3O_3$	Citrulline
78	C	203.150	0.006±0.002	0.007±0.002	0.010±0.005	0.0004	$C_8H_{18}N_4O_2$	SDMA
82	C	209.093	0.010±0.004	0.011±0.005	0.016±0.005	0.0002	$C_{10}H_{12}N_2O_3$	Kynurenine
96	C	243.184	0.026±0.013	0.019±0.012	0.015±0.007	0.0301		
97	C	244.106	0.0006±0.001	0.0009±0.001	0.002±0.002	0.0003		
114	C	276.128	0.008±0.006	0.006±0.004	0.003±0.003	0.0104		
127	C	302.197	0.106±0.050	0.079±0.047	0.062±0.028	0.0372		
134	C	316.213	0.010±0.009	0.006±0.007	0.003±0.002	0.0158		
152	A	96.960	0.216±0.063	0.243±0.063	0.341±0.103	<0.0001		
158	A	103.014	0.003±0.002	0.004±0.002	0.005±0.002	0.0001	$C_2H_4N_2O_3$	
202	A	149.049	0.030±0.006	0.034±0.009	0.051±0.019	<0.0001	$C_6H_6N_4O$	
232	A	187.098	0.020±0.013	0.017±0.011	0.009±0.004	<0.0001	$C_9H_{16}O_4$	Azelaic acid
246	A	209.031	0.029±0.012	0.024±0.009	0.016±0.013	<0.0001	$C_6H_{10}O_8$	Galactaric acid

[a] Mode "C" and "A" indicate that the candidate metabolites were obtained in cationic and anionic analysis, respectively
The relative ratio of peak area of each metabolite is shown as the mean±SD

$0.792\pm1.21\times10^{-2}$) in the cross-validation test. In a bootstrap test, the AUCs were 0.875±0.0419 and 0.820±0.0543 for training and cross-validation, respectively. These results indicate that the developed model is sufficiently accurate, specific, and general.

Table 3 AUC values for individual markers

Metabolite	AUC	95 % CI		*p* value
Creatinine	0.7526	0.6423	0.8629	8.06×10^{-4}
MID 17	0.7319	0.6128	0.851	2.09×10^{-3}
Aspartic acid	0.7069	0.5871	0.8267	6.05×10^{-3}
γ–Butyrobetaine	0.7379	0.6149	0.8609	1.60×10^{-3}
MID 51	0.644	0.5021	0.7858	0.0561
MID 52	0.7078	0.5853	0.8302	5.84×10^{-3}
Citrulline	0.6431	0.5158	0.7704	0.0576
SDMA	0.731	0.6098	0.8522	2.18×10^{-3}
Kynurenine	0.7284	0.6122	0.8447	2.44×10^{-3}
MID 96	0.6828	0.5475	0.818	0.0153
MID 97	0.6655	0.5396	0.7914	0.0281
MID 114	0.6836	0.5399	0.8274	0.0148
MID 127	0.6707	0.5321	0.8093	0.0235
MID 134	0.6552	0.5102	0.8001	0.0395
MID 152	0.7302	0.6048	0.8555	2.26×10^{-3}
MID 158	0.7108	0.5809	0.8407	5.16×10^{-3}
MID 202	0.7647	0.6492	0.8801	4.47×10^{-4}
Azelaic acid	0.731	0.6151	0.8469	2.18×10^{-3}
Galactaric acid	0.7591	0.6169	0.9012	5.89×10^{-4}

Discussion

The aim of this study was to obtain metabolic markers for early detection of DN from patient serum samples. We used CE-MS-based metabolome analysis to find differences in the serum metabolites from non-DN, micro-DN, and macro-DN samples. OPLS-DA with 289 metabolites clearly separated non-DN from macro-DN. Adequate separation of micro-DN from non-DN was also achieved. These results show that OPLS-DA is useful in this type of analysis. The resultant S-plot of the developed OPLS-DA model identified 19 metabolites that were major contributors to the separation of macro-DN from non-DN ($|p(corr)|>0.5$). These metabolites showed a gradual increase or decrease with progressive development of nephropathy. Among them, eight metabolites were identified, and these markers are discussed in comparison with other published reports below.

The concentration of serum creatinine was significantly increased in the micro-DN and macro-DN groups compared with the non-DN group ($p<0.0001$), and positively correlated with UACR ($r=0.5701$, $p<0.0001$) and negatively correlated

Table 4 Correlation analysis between the 19 biomarker candidates and clinical parameters (urinary albumin-to-creatinine ratio (UACR) or estimated glomerular filtration rate (eGFR))

MID	Metabolite	UACR		eGFR	
		Coefficients	*p* value	Coefficients	*p* value
11	Creatinine	0.5701	<0.0001[a]	−0.8832	<0.0001[a]
17		0.4968	<0.0001[a]	−0.5808	<0.0001[a]
29	Aspartic acid	0.4993	<0.0001[a]	−0.3912	0.0004[a]
39	γ-Butyrobetaine	0.4942	<0.0001[a]	−0.6492	<0.0001[a]
51		0.4728	<0.0001[a]	0.2204	<0.0001[a]
52		−0.4871	<0.0001[a]	−0.0678	0.053
69	Citrulline	0.4300	<0.0001[a]	−0.6531	<0.0001[a]
78	SDMA	0.4820	<0.0001[a]	−0.7111	<0.0001[a]
82	Kynurenine	0.5351	<0.0001[a]	−0.5627	<0.0001[a]
96		−0.3085	0.006[b]	0.1975	0.083
97		0.5223	<0.0001[a]	−0.7651	<0.0001[a]
114		−0.3638	0.001[b]	0.1392	0.224
127		−0.2961	0.009[b]	0.2035	0.074
134		−0.3669	0.001[a]	0.2397	0.035[c]
152		0.5336	<0.0001[a]	−0.7687	<0.0001[a]
158		0.4980	<0.0001[a]	−0.6302	<0.0001[a]
202		0.6352	<0.0001[a]	−0.7455	<0.0001[a]
232	Azelaic acid	−0.5210	<0.0001[a]	0.3739	0.0007[a]
246	Galactaric acid	−0.4596	<0.0001[a]	0.4152	0.0002[a]

[a] $p<0.001$
[b] $p<0.01$
[c] $p<0.05$

with eGFR ($r=-0.8832$, $p<0.0001$). Accumulation of serum creatinine was also observed in DN patients by metabolic analysis [19]. In clinical practice, creatinine is widely used as a marker of DN that reflects the renal function. Although serum creatinine had high specificity for detecting decreased GFR, the sensitivity is not sufficient because its levels do not significantly increase until the GFR is reduced to less than 50 % of normal levels [20].

The levels of amino acids, including aspartic acid ($p<0.0001$), citrulline ($p=0.0005$), SDMA ($p=0.0004$), and kynurenine ($p=0.0002$), were significantly elevated in the DN groups compared with the non-DN group. These metabolites showed high positive correlations with UACR (aspartic acid, $r=0.4993$, $p<0.0001$; citrulline, $r=0.4300$, $p<0.0001$; SDMA, $r=0.4820$, $p<0.0001$; kynurenine, $r=0.5351$, $p<0.0001$) and negative correlations with eGFR (aspartic acid, $r=-0.3912$, $p=0.0004$; citrulline, $r=-0.6531$, $p<0.0001$; SDMA, $r=-0.7111$, $p<0.0001$; kynurenine, $r=-0.5627$, $p<0.0001$). Aspartic acid and citrulline are involved in the urea cycle. Urea, is a major end product of

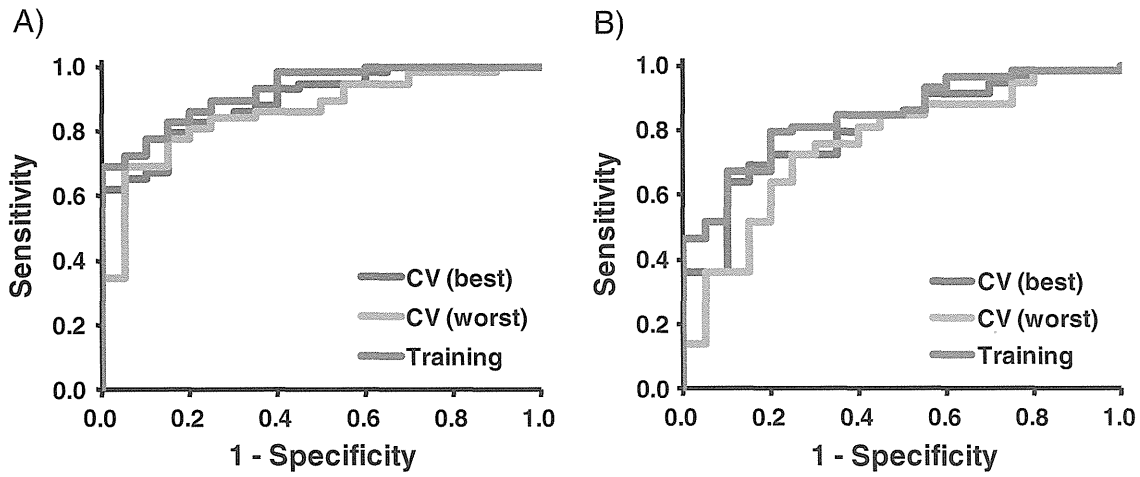

Fig. 2 ROC curve analyses in combination with (**A**) γ-butyrobetaine, SDMA, azelaic acid, MID 114, and MID 127, and (**B**) aspartic acid, SDMA, azelaic acid, and galactaric acid to discriminate non-DN and DN patients

nitrogen metabolism, and is produced by free ammonia and aspartic acid. Citrulline is normally taken up by the kidneys and converted to urea via arginine. Chuang et al. found significant accumulation of urea cycle intermediates in the patients with end-stage renal disease [21]. Because the kidneys are important in conversion of citrulline to arginine, the increase in the serum level of citrulline in DN patients could be attributed to degradation of this function.

SDMA and asymmetric dimethylarginine (ADMA), which is a structural isomer of SDMA, are formed by the enzymatic methylation of arginine residues within proteins. These metabolites have been identified as biomarkers for chronic kidney disease [22]. ADMA is metabolized by dimethylarginine dimethylaminohydrolase (EC 3.5.3.18) into citrulline and dimethylamine in the kidneys, whereas SDMA is excreted directly into the urine without further modification [23]. In this study, ADMA was under the detection limit, but SDMA was positively correlated with a decrease in function of kidney. Therefore, SDMA is a more sensitive marker than ADMA of various renal diseases, including DN.

Tryptophan is metabolized to kynurenine and further metabolized to acetyl-CoA and NAD in the tryptophan-kynurenine pathway. The rate limiting enzymes of this pathway are indoleamine 2,3-dioxygenase (EC 1.13.11.52) in the kidney and tryptophan 2,3-dioxygenase (EC 1.13.11.11) in the liver. Both these enzymes metabolize tryptophan to *N*-formylkynurenine, and *N*-formylkynurenine is subsequently catabolized to kynurenine. Saito et al. showed the peripheral kynurenine pathway accelerates in renal insufficient rats, and the reaction rate was positively correlated with the severity of the case [24]. They also found increased serum kynurenine concentrations reflected increased tryptophan 2,3-dioxygenase and decreased kynureninase (EC 3.7.1.3) activity in the liver [24]. Integration of profiling of these enzyme activities and metabolites will increase understanding of these mechanisms.

We detected a significant increase in γ-butyrobetaine in DN patients ($p<0.0001$). Toyohara et al. showed a negative correlation between γ-butyrobetaine and eGFR in plasma from the patients with chronic kidney disease [25]. Because γ-butyrobetaine is converted to L-carnitine by γ-butyrobetaine dioxygenase (EC 1.14.11.1), it is assumed the increased γ-butyrobetaine arises from inhibition of this enzyme in the kidney.

The levels of azelaic acid ($p<0.0001$) and galactaric acid ($p<0.0001$) were significantly lower in the DN groups than the non-DN group. These metabolites also showed high negative correlations with UACR (azelaic acid, $r=-0.5210$, $p<0.0001$; galactaric acid, $r=-0.4596$, $p<0.0001$) and positive correlations with eGFR (azelaic acid, $r=0.3739$, $p=0.0007$; galactaric acid, $r=0.4152$, $p=0.0002$). Azelaic acid is a saturated C9 dicarboxylic acid derived from oxidation of fatty acids and inhibits the generation of reactive oxygen species on neutrophils [26]. Galactaric acid, is a natural product found in various fruits, and acts as a growth substrate for many organisms, including *Escherichia coli* [27]. However, biological mechanisms of decreased serum azelaic acid and galactaric acid after onset DN need to be clarified.

In this study, the obtained 19 metabolites showed relatively high separation abilities (AUC values of receiver operating characteristic curves 0.643–0.765, Table 3). To increase the separation ability, we then applied a MLR model to this dataset. The developed MLR model included five metabolites, γ-butyrobetaine, SDMA, azelaic acid, MID 114, and MID 127. This model had a higher AUC value for diagnosis of DN (0.927, $p<0.0001$) than single markers, and shows the use of multiple markers is advantageous (Fig. 2a). However, this model contained two unidentified metabolites. The model using only identified metabolites was even simpler and more versatile for actual diagnosis because it could be used with quantification by another technique, such as LC, LC-MS, or an enzymatic method. Thus, we developed another MLR model using only the identified metabolites, aspartic acid, SDMA, azelaic acid and galactaric acid (Fig. 2b). This model showed high separation ability (AUC value 0.844, $p<0.0001$), and could also be used to diagnose DN. However, there are several limitations to be acknowledged for this study. For example, the developed model should be further validated using larger and independent new datasets. In addition, although we evaluated the generalization ability of the developed model using cross-validation, the specificity of the model was not assessed. Especially, the specificity for DN using data obtained from study of other kidney diseases (e.g., kidney cancer) should be addressed in future study.

In conclusion, we applied CE-MS-based metabolome profiling to serum samples from diabetic patients with or without existing DN. Biomarker candidates for the early diagnosis of DN were obtained. Although a further validation study is needed, this technique has potential as a tool for biomarker discovery studies.

Acknowledgments We thank Dr. Astuko Watarai, Japan Labour Health and Welfare Organization Chubu Rosai Hospital, for assistance with sample collection. We also thank Maki Sugawara and Hiroko Ueda, Institute for Advanced Biosciences, Keio University, and Jiro Nakamura, Department of Endocrinology and Diabetes, Nagoya University Graduate School of Medicine, for technical support and fruitful discussions. This work was supported by a Health and Labour Sciences Research Grant "Research on Biological Markers for New Drug Development", Grants from the Ministry of Health, Labour and Welfare of Japan "Research on Rare and Intractable Disease", KAKENHI Grants-in-Aid for Scientific Research on Priority Areas "Systems Genomes" and "Lifesurveyor" from the Ministry of Education, Culture, Sports, Science and Technology of Japan, and research funds from the Yamagata prefectural government and the City of Tsuruoka.

References

1. Gross JL, de Azevedo MJ, Silveiro SP, Canani LH, Caramori ML, Zelmanovitz T (2005) Diabetic nephropathy: diagnosis, prevention, and treatment. Diabetes Care 28(1):164–176
2. Kim HJ, Cho EH, Yoo JH, Kim PK, Shin JS, Kim MR, Kim CW (2007) Proteome analysis of serum from type 2 diabetics with nephropathy. J Proteome Res 6(2):735–743
3. Molitch ME, DeFronzo RA, Franz MJ, Keane WF, Mogensen CE, Parving HH, Steffes MW (2004) Nephropathy in diabetes. Diabetes Care 27(Suppl 1):S79–S83
4. Tabaei BP, Al-Kassab AS, Ilag LL, Zawacki CM, Herman WH (2001) Does microalbuminuria predict diabetic nephropathy? Diabetes Care 24(9):1560–1566
5. Dihazi H, Muller GA, Lindner S, Meyer M, Asif AR, Oellerich M, Strutz F (2007) Characterization of diabetic nephropathy by urinary proteomic analysis: identification of a processed ubiquitin form as a differentially excreted protein in diabetic nephropathy patients. Clin Chem 53(9):1636–1645
6. Mischak H, Kaiser T, Walden M, Hillmann M, Wittke S, Herrmann A, Knueppel S, Haller H, Fliser D (2004) Proteomic analysis for the assessment of diabetic renal damage in humans. Clin Sci (Lond) 107(5):485–495
7. Tiziani S, Lopes V, Gunther UL (2009) Early stage diagnosis of oral cancer using 1H NMR-based metabolomics. Neoplasia 11(3):269–276
8. Kind T, Tolstikov V, Fiehn O, Weiss RH (2007) A comprehensive urinary metabolomic approach for identifying kidney cancer. Anal Biochem 363(2):185–195
9. Sieber M, Wagner S, Rached E, Amberg A, Mally A, Dekant W (2009) Metabonomic study of ochratoxin a toxicity in rats after repeated administration: phenotypic anchoring enhances the ability for biomarker discovery. Chem Res Toxicol 22(7):1221–1231
10. Hirayama A, Kami K, Sugimoto M, Sugawara M, Toki N, Onozuka H, Kinoshita T, Saito N, Ochiai A, Tomita M, Esumi H, Soga T (2009) Quantitative metabolome profiling of colon and stomach cancer microenvironment by capillary electrophoresis time-of-flight mass spectrometry. Cancer Res 69(11):4918–4925
11. Soga T, Baran R, Suematsu M, Ueno Y, Ikeda S, Sakurakawa T, Kakazu Y, Ishikawa T, Robert M, Nishioka T, Tomita M (2006) Differential metabolomics reveals ophthalmic acid as an oxidative stress biomarker indicating hepatic glutathione consumption. J Biol Chem 281(24):16768–16776
12. Sugimoto M, Wong DT, Hirayama A, Soga T, Tomita M (2010) Capillary electrophoresis mass spectrometry-based saliva metabolomics identified oral, breast and pancreatic cancer-specific profiles. Metabolomics 6(1):78–95
13. Xia JF, Liang QL, Hu P, Wang YM, Li P, Luo GA (2009) Correlations of six related purine metabolites and diabetic nephropathy in Chinese type 2 diabetic patients. Clin Biochem 42(3):215–220
14. Jiang Z, Liang Q, Luo G, Hu P, Li P, Wang Y (2009) HPLC-electrospray tandem mass spectrometry for simultaneous quantitation of eight plasma aminothiols: application to studies of diabetic nephropathy. Talanta 77(4):1279–1284
15. Zhang J, Yan L, Chen W, Lin L, Song X, Yan X, Hang W, Huang B (2009) Metabonomics research of diabetic nephropathy and type 2 diabetes mellitus based on UPLC-oaTOF-MS system. Anal Chim Acta 650(1):16–22
16. Soga T, Ohashi Y, Ueno Y, Naraoka H, Tomita M, Nishioka T (2003) Quantitative metabolome analysis using capillary electrophoresis mass spectrometry. J Proteome Res 2(5):488–494
17. Soga T, Igarashi K, Ito C, Mizobuchi K, Zimmermann HP, Tomita M (2009) Metabolomic profiling of anionic metabolites by capillary electrophoresis mass spectrometry. Anal Chem 81(15):6165–6174
18. Witten I, Frank E (2000) Data mining: practical machine learning algorithms with Java implementations. Morgan Kaufmann Publishers, CA
19. Xia JF, Liang QL, Liang XP, Wang YM, Hu P, Li P, Luo GA (2009) Ultraviolet and tandem mass spectrometry for simultaneous quantification of 21 pivotal metabolites in plasma from patients with diabetic nephropathy. J Chromatogr B Analyt Technol Biomed Life Sci 877(20–21):1930–1936
20. Perrone RD, Madias NE, Levey AS (1992) Serum creatinine as an index of renal function: new insights into old concepts. Clin Chem 38(10):1933–1953
21. Chuang CK, Lin SP, Chen HH, Chen YC, Wang TJ, Shieh WH, Wu CJ (2006) Plasma free amino acids and their metabolites in Taiwanese patients on hemodialysis and continuous ambulatory peritoneal dialysis. Clin Chim Acta 364(1–2):209–216
22. Fleck C, Janz A, Schweitzer F, Karge E, Schwertfeger M, Stein G (2001) Serum concentrations of asymmetric (ADMA) and symmetric (SDMA) dimethylarginine in renal failure patients. Kidney Int 59:S14–S18
23. Pahlich S, Zakaryan RP, Gehring H (2006) Protein arginine methylation: cellular functions and methods of analysis. Biochim Biophys Acta 1764(12):1890–1903
24. Saito K, Fujigaki S, Heyes MP, Shibata K, Takemura M, Fujii H, Wada H, Noma A, Seishima M (2000) Mechanism of increases in L-kynurenine and quinolinic acid in renal insufficiency. American Journal of Physiology-Renal Physiology 279(3):F565
25. Toyohara T, Akiyama Y, Suzuki T, Takeuchi Y, Mishima E, Tanemoto M, Momose A, Toki N, Sato H, Nakayama M, Hozawa A, Tsuji I, Ito S, Soga T, Abe T (2010) Metabolomic profiling of uremic solutes in CKD patients. Hypertens Res 33 (9):944–952
26. Akamatsu H, Komura J, Asada Y, Miyachi Y, Niwa Y (1991) Inhibitory effect of azelaic acid on neutrophil functions: a possible cause for its efficacy in treating pathogenetically unrelated diseases. Arch Dermatol Res 283(3):162–166
27. Watanabe S, Yamada M, Ohtsu I, Makino K (2007) α-Ketoglutaric semialdehyde dehydrogenase isozymes involved in metabolic pathways of D-glucarate, D-galactarate, and hydroxy-L-proline. J Biol Chem 282(9):6685

Macrophage-mediated glucolipotoxicity via myeloid-related protein 8/toll-like receptor 4 signaling in diabetic nephropathy

Takashige Kuwabara, Kiyoshi Mori, Masashi Mukoyama, Masato Kasahara, Hideki Yokoi & Kazuwa Nakao

Clinical and Experimental Nephrology
Official Publication of the Japanese Society of Nephrology

ISSN 1342-1751

Clin Exp Nephrol
DOI 10.1007/s10157-013-0922-5

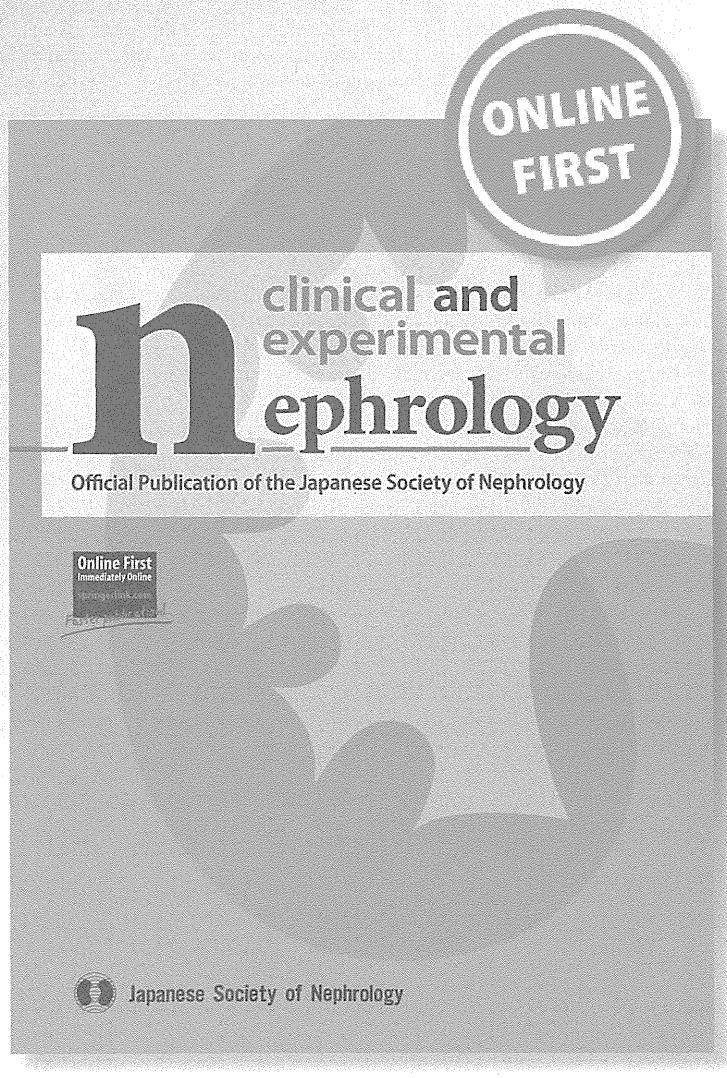

Springer

Clin Exp Nephrol
DOI 10.1007/s10157-013-0922-5

REVIEW ARTICLE

Macrophage-mediated glucolipotoxicity via myeloid-related protein 8/toll-like receptor 4 signaling in diabetic nephropathy

Takashige Kuwabara · Kiyoshi Mori · Masashi Mukoyama · Masato Kasahara · Hideki Yokoi · Kazuwa Nakao

Received: 16 April 2013 / Accepted: 28 November 2013

Abstract Dyslipidemia is an independent risk factor for the development and progression of diabetic nephropathy (DN). In this review, we summarize mouse models with both diabetes and dyslipidemia, and their associated complications. We then discuss molecules potentially involved in deterioration of DN by dyslipidemia. We focus especially upon toll-like receptor 4 (TLR4) and one of its endogenous ligands, myeloid-related protein 8 (MRP8 or S100A8), since we have found that their mRNA levels are commonly increased in glomeruli of type 1 (streptozotocin [STZ]-induced) and type 2 (*A-ZIP/F-1* lipoatrophic) diabetic mice. Gene expression of *MRP8* and *Tlr4* is further upregulated during worsening of STZ-induced DN by a high fat diet (HFD). Moreover, these HFD-induced changes are accompanied by enhanced gene expression of *CCAAT element binding protein β* and phosphorylation of c-Jun N-terminal kinase in the kidney, which have also been reported in pancreatic β cells under diabetic-hyperlipidemic conditions. Effects of a HFD upon DN are cancelled in *Tlr4* knockout mice. Macrophages are the predominant source of MRP8 in glomeruli. In cultured macrophages, combinatorial treatment with high glucose and palmitate amplifies *MRP8* expression in a *Tlr4*-dependent manner, and recombinant MRP8 protein markedly increases gene expression of the inflammatory cytokines *interleukin-1β* and *tumor necrosis factor α*. Here, we propose 'macrophage-mediated glucolipotoxicity' via activation of MRP8/TLR4 signaling as a novel mechanism of pathophysiology for DN.

Keywords Diabetic nephropathy · Glucolipotoxicity · Macrophage · Toll-like receptor

Introduction

Since only one-third of patients with type 1 diabetes develop diabetic nephropathy (DN), we should consider the role of factors other than hyperglycemia in the pathophysiology of DN, including genetic, epigenetic, environmental and metabolic aspects. Several reports describe hyperlipidemia or dyslipidemia as an independent risk factor for the progression of DN in type 1 and type 2 diabetes, as well as for atherosclerotic complications [1–4]. Using type 1 (streptozotocin [STZ]-induced) and type 2 (*db/db*) diabetic mouse models, we have confirmed that treatment of diabetic mice with a high fat diet (HFD) exacerbates albuminuria and glomerular lesions [5]. Of note, single nucleotide polymorphisms in *acetyl-CoA carboxylase β* gene, which plays an important role in the regulation of fatty acid metabolism, exhibit a potent association with proteinuria in patients with type 2 diabetes [6, 7]. Accordingly, a concept of synergistic toxicity caused

This article was, in part, presented at the 43rd Western Regional Meeting of the Japanese Society of Nephrology, held at Matsuyama, Japan, in 2013.

T. Kuwabara · K. Mori (✉) · M. Mukoyama · M. Kasahara · H. Yokoi · K. Nakao
Department of Medicine and Clinical Science, Kyoto University Graduate School of Medicine, Kyoto University Hospital, Kyoto 606-8507, Japan
e-mail: keyem@kuhp.kyoto-u.ac.jp

K. Mori
Medical Innovation Center, Kyoto University Graduate School of Medicine, Kyoto 606-8507, Japan

M. Kasahara
Department of EBM Research, Institute for Advancement of Clinical and Translational Science, Kyoto University Hospital, Kyoto, Japan

Published online: 20 December 2013

by glucose and lipid, described as 'glucolipotoxicity', has emerged in recent years. However, the underlying molecular mechanism is still obscure, especially in renal complication [8]. Here we will discuss diabetic-hyperlipidemic mouse models and glucolipotoxicity in the kidney.

Diabetic-hyperlipidemic mouse models

As described above, several clinical and experimental phenomena have highlighted the synergistic effects of hyperglycemia and hyperlipidemia upon the development and progression of diabetic complications including nephropathy. Despite the fact that there are several limitations associated with the difference in hyperlipidemia between rodents and humans, mouse models are still most widely used to study complications caused by diabetes and hyperlipidemia. The reasons include small animal size, short generation time, the ease of induction of diabetes, hyperlipidemia or gene manipulation, and cost effectiveness [9]. Hence, in the last decade diabetic-hyperlipidemic mouse models have been used for genetic modification, pharmacological treatment and/or some particular chow diets that abundantly contain fat and/or cholesterol. In this section, representative mouse models are summarized.

Apolipoprotein E-deficient mice treated with streptozotocin (*ApoE* KO + STZ)

ApoE KO + STZ mice are one of the most popular diabetic-hyperlipidemic mouse models. This model shows not only hypercholesterolemia and hypertriglyceridemia, but also accelerated aortic atherosclerotic lesions [10–12] and nephropathy [13–15] associated with diabetes. These reports revealed that advanced glycation end-products [13, 14] and endoplasmic reticulum (ER) stress [16, 17] are candidate mediators of glucolipotoxicity in *ApoE* KO + STZ mice.

Low-density lipoprotein (LDL) receptor-deficient mice treated with STZ (*LDLR* KO + STZ)

LDLR KO + STZ mice show dyslipidemia including high LDL cholesterol, low high-density lipoprotein (HDL) cholesterol levels and hypertriglyceridemia, mimicking human metabolic syndrome [18]. Moreover, addition of a HFD exacerbates hypertriglyceridemia, hypercholesterolemia, and diabetic renal lesions (including glomerular and tubulointerstitial macrophage infiltration) in this model [19]. The authors [19] referred to an earlier work indicating that irradiation-induced depletion of bone marrow cells (including monocytes) reduces renal injury in STZ-diabetic rats [20].

STZ-induced diabetic mice with HFD feeding (STZ + HFD)

A supplemental HFD on STZ-treated diabetic mice increases blood triglyceride and free fatty acid concentrations, at least in part, because of insulin deficiency, suggesting that this model might be useful especially for analyzing pathophysiology by high triglyceride-rich lipoprotein and/or high free fatty acids coexisting with high glucose conditions. In STZ + HFD mice, there are several reports describing vascular complications such as cardiovascular dysfunction [21], retinopathy [22], neuropathy [23] and nephropathy [5, 24].

Treatment of wild-type mice with STZ and HFD synergistically increases albuminuria [5] and expands mesangial area (Fig. 1). Induction of diabetes by STZ causes a marked increase in urine volume and creatinine clearance of normal diet-fed and HFD-fed animals, respectively, suggesting that glomerular hyperfiltration has occurred. On the other hand, HFD treatment reduces urine volume and creatinine clearance in STZ mice (Fig. 1), suggesting that HFD is not causing more hyperfiltration but is causing non-hemodynamic actions which will be discussed below.

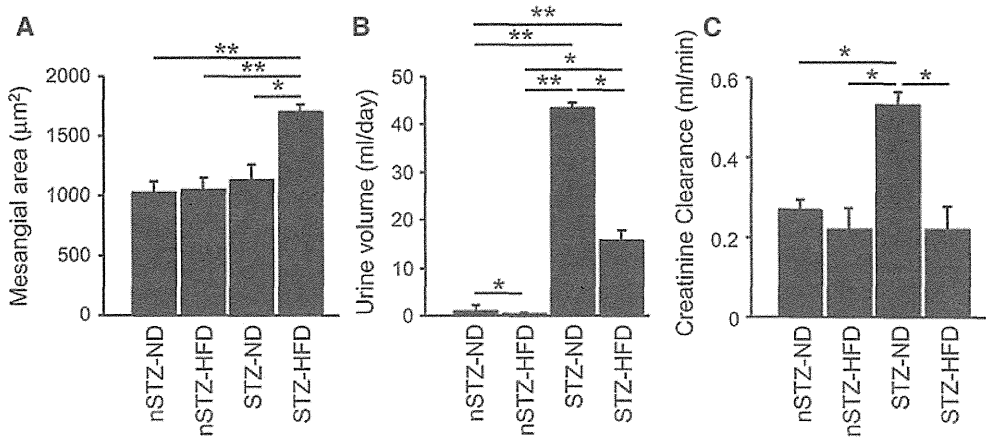

Fig. 1 Effects of STZ and/or HFD upon mesangial expansion (**a**), urine volume (**b**) and creatinine clearance (**c**) in wild-type mice. *nSTZ-ND* non STZ-normal diet, *nSTZ-HFD* non STZ-high fat diet, *STZ-ND* STZ-normal diet, *STZ-HFD* STZ-high fat diet. Data are mean ± SEM. $n = 4$–11. $^{*}p < 0.01$, $^{**}p < 0.001$. Modified from Kuwabara and others [5]

A-ZIP/F-1 lipoatrophic diabetic mice

A-ZIP/F-1 mice are a genetic mouse model of lipoatrophic diabetes, characterized by severe insulin resistance, dyslipidemia including hypertriglyceridemia and high free fatty acids, and fatty liver [25, 26]. This model is based upon dominant-negative expression of B-ZIP transcription factors of both C/EBP and Jun families under the control of aP2 enhancer/promoter, causing paucity of adipose tissue. *A-ZIP/F-1* mice may serve as a useful tool for studying DN, because they manifest severe nephrotic syndrome and typical histopathological renal lesions which are glomerular hypertrophy, diffuse and pronounced mesangial expansion and accumulation of extracellular matrix [27]. Notably, these renal changes are reversible to some extent by replacement therapy with a fat-derived hormone leptin [27].

Other mouse models

There are a few other diabetic-hyperlipidemic mouse models such as non-obese diabetic mice or $Ins2^{Akita}$ diabetic mice combined with HFD feeding [28, 29], but their renal involvement has not been characterized well. Regardless of the models described above, differences in genetic backgrounds critically affect glucose and lipid metabolism among mouse strains [30]. Furthermore, even similar levels of hyperglycemia cause distinct renal changes among different strains and species. For instance, the DBA/2 strain is highly susceptible to DN, whereas the C57BL/6 strain is relatively resistant [31–33]. In addition, since cholesteryl ester transfer protein is inactive in rodents, HDL is the dominant lipoprotein in mice [34]. Apolipoprotein B in rodents also differs from that in humans [35].

Molecules involved in glucolipotoxicity in the kidney and pancreatic β cells

Although glucotoxicity and lipotoxicity were originally proposed as independent concepts, Prentki et al. reported a novel concept of glucolipotoxicity in pancreatic β cells in 1996. They reported that elevated ambient levels of glucose and free fatty acid cause synergistic inhibition of insulin secretion [36]. On the other hand, they reported that increased intracellular glucose-derived metabolites inhibit enzymes for β-oxidation, leading to cytosolic accumulation of lipids [37]. Subsequently, there have been several reports about the molecular mechanism underlying glucolipotoxicity involved in pancreatic β cell dysfunction and insulin resistance [38–40]. Furthermore, phenomena of glucolipotoxicity are also observed in DN of humans [1–4] and rodents [41, 42], but their pathophysiology remains largely unknown [8]. Here, we will compare glucolipotoxicity upon pancreatic β cell dysfunction and DN.

c-Jun N-terminal kinase (JNK)

JNK plays a pivotal role in ER stress-induced 'unfolded protein response' in innate immune system [43]. It was later revealed that ER stress-induced JNK activation is associated with chronic inflammation or high ambient fatty acid levels in obesity or type 2 diabetes [44, 45]. In pancreatic β-cells, high glucose concentrations augment lipotoxicity through JNK activation, at least partly, in an ER stress-dependent manner [46, 47]. In our diabetic-hyperlipidemic model [5], treatment with STZ and HFD synergistically increases phosphorylation of IκB and mRNA expression of pro-inflammatory genes in the kidney, in parallel with phosphorylation of JNK, but not with phosphorylation of other mitogen-activated protein (MAP) kinases such as p38 or extracellular signal-regulated kinase (ERK) (Fig. 2).

CCAAT element binding protein beta (C/EBPβ)

CCAAT element binding protein beta (C/EBPβ) is one of the transcriptional repressors of insulin gene and induced

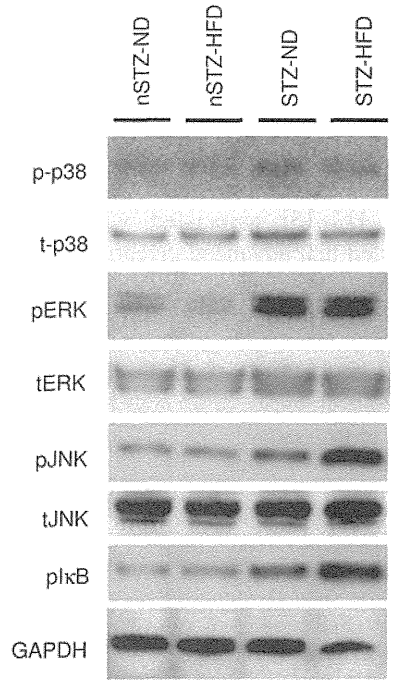

Fig. 2 Western blot analysis for phosphorylation of MAP kinases and IκB in kidney of STZ + HFD mice. *p-/t-p38* phosphorylated/total p38 MAP kinase, *p/tERK* phosphorylated/total extracellular signal-regulated kinase, *p/tJNK* phosphorylated/total c-Jun N-terminal kinase, *pIκB* phosphorylated inhibitor of κB. Modified from Kuwabara and others [5]

by chronic hyperglycemia [48]. C/EBPβ is increased by fatty acids through the Per-Arnt-Sim kinase (PASK) pathway [49] in pancreatic β cells. Since PASK is also induced by high glucose conditions, these mechanisms may possibly exert glucolipotoxic effects. In the kidney, C/EBPβ is increased in diabetic rats, but not other C/EBP isoforms [50]. Furthermore, renal upregulation of *C/EBPβ* mRNA in STZ-induced diabetic mice is further enhanced by additional HFD feeding in our experiments [5].

Of note, JNK/AP-1 and C/EBPβ pathways may also contribute to glucolipotoxicity-induced renal damage through upregulation of myeloid-related protein 8 (MRP8, also known as S100A8 or calgranulin A), whose gene promoter region contains AP-1 binding site [51, 52] and C/EBP motif [53, 54], as discussed in the next section.

Fetuin A

Over the last few years, there has been growing evidence for fatty acid-induced lipotoxicity, such as insulin resistance, through toll-like receptor 4 (TLR4) [55–57]. However, it is still controversial whether fatty acid stimulates TLR4 directly or indirectly. Recently, fetuin A has been identified as an adopter protein combining fatty acids and TLR4 [58], and its plasma levels are elevated in diabetic humans and mice [59, 60]. ER stress induced by high glucose and palmitate increases the expression of fetuin A [60], suggesting that fetuin A could hypothetically participate in glucolipotoxicity upon macrophages.

MRP8/TLR4

MRP8 was originally identified as a cytoplasmic calcium-binding protein in neutrophils and monocytes [61]. MRP8, by making a heterodimer with MRP14 (or S100A9), has become widely recognized as a potent endogenous ligand for TLR4 in various diseases including septic shock and vascular and autoimmune disorders [62–64]. To identify candidate disease-modifying molecules in DN, we have performed microarray analysis using isolated glomeruli from two different diabetic models of mice—STZ-induced insulin-dependent diabetic mice and lipoatrophic insulin-resistant A-ZIP/F-1 mice. We then focused upon *MRP8* and *Tlr4*, because expression of both genes is commonly increased in these two models [5]. It is noteworthy that diabetic-hyperlipidemic mice such as STZ-HFD mice or *A-ZIP/F-1* mice show remarkable upregulation of *MRP8* and *Tlr4* compared to control non-diabetic mice (Fig. 3). Since macrophages are identified as the major source of MRP8 in the glomeruli of STZ-HFD mice [5], we examined the effects of high glucose and fatty acid on the expression of *MRP8* (Fig. 4) and *Tlr4* in cultured macrophages. This in vitro study showed that treatment with fatty acid

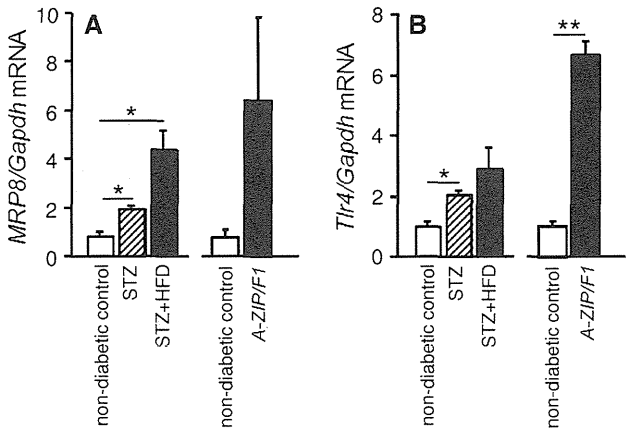

Fig. 3 Glomerular gene expression of *MRP8* (**a**) and *Tlr4* (**b**) in STZ + HFD and lipoatrophic *A-ZIP/F-1* mice determined by TaqMan real-time PCR. *White bars* non-diabetic control group, *striped bars* diabetic group, *black bars* diabetic-hyperlipidemic group. Data are mean ± SEM. $n = 4$–7. $^{*}p < 0.01$, $^{**}p < 0.001$. Modified from Kuwabara and others [5]

amplifies *MRP8* expression only under high ambient glucose conditions. Although *Tlr4* is expressed slightly more in high glucose conditions than in low glucose conditions, fatty acid does not alter *Tlr4* expression [5]. In addition, synergistic effects with high glucose and fatty acid on macrophages and diabetic kidneys are abrogated by *Tlr4* deletion [5] (Fig. 4). Moreover, we have observed that recombinant MRP8 protein markedly increases gene expression of the inflammatory cytokines *interleukin-1β* and *tumor necrosis factor α* (*TNF-α*) in cultured macrophages (submitted) [62]. Similarly, macrophages also play an important role in insulin resistance and β-cell dysfunction through fatty acid-induced TLR4 activation [65, 66]. Particularly in the kidney, MRP8 produced by infiltrated macrophages might exert glucolipotoxic effects upon diabetic glomeruli in a paracrine manner, potentially leading to mesangial expansion, podocyte injury, glomerular sclerosis and albuminuria (Fig. 5), because TLR4 is reportedly expressed in healthy or injured glomerular intrinsic cells including mesangial cells [67, 68], endothelial cells [67, 69] and podocytes [70, 71]. Taken together, we propose 'macrophage-mediated glucolipotoxicity' via activation of MRP8/TLR4 signaling as a novel concept for pathophysiology of DN (Fig. 5).

To understand the clinical implication of MRP8 expression in humans, we have carried out immunohistochemical analysis of MRP8 expression in renal biopsy samples from patients with DN, obesity-related glomerulopathy (ORG) and non-obese, non-diabetic controls (which are minor glomerular abnormality [MGA] and minimal change nephrotic syndrome [MCNS]). We have not been able to obtain reliable antibody against TLR4 to date. The rank orders of glomerular and tubulointerstitial MRP8 protein expression levels

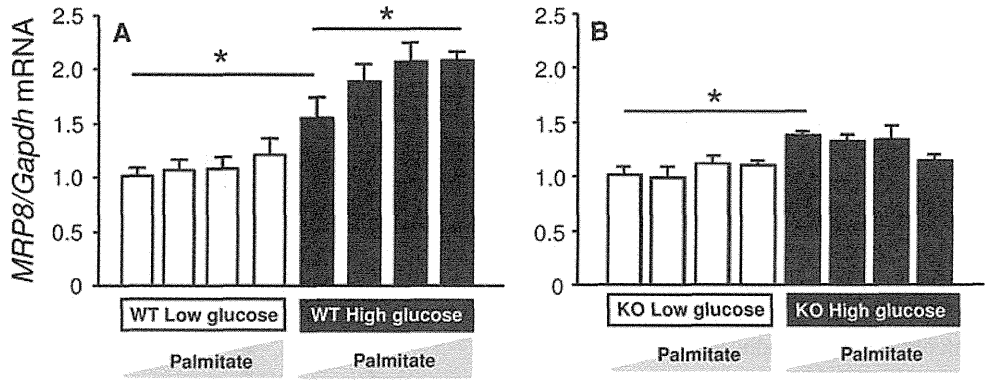

Fig. 4 Gene expression of *MRP8* and effects of glucose or fatty acid in bone marrow-derived macrophages (BMDMs) determined by TaqMan real-time PCR. BMDMs generated from wild-type (WT, **a**) or *Tlr4* knockout (KO, **b**) mice were cultured under low-glucose (100 mg/dl, *white bars*) or high-glucose (450 mg/dl, *black bars*) conditions, and were stimulated with palmitate (0, 10, 50, and 200 μM, respectively, from the *left*) for 24 h. Data are mean ± SEM. $n = 6$. $^*p < 0.05$. Modified from Kuwabara and others [5]

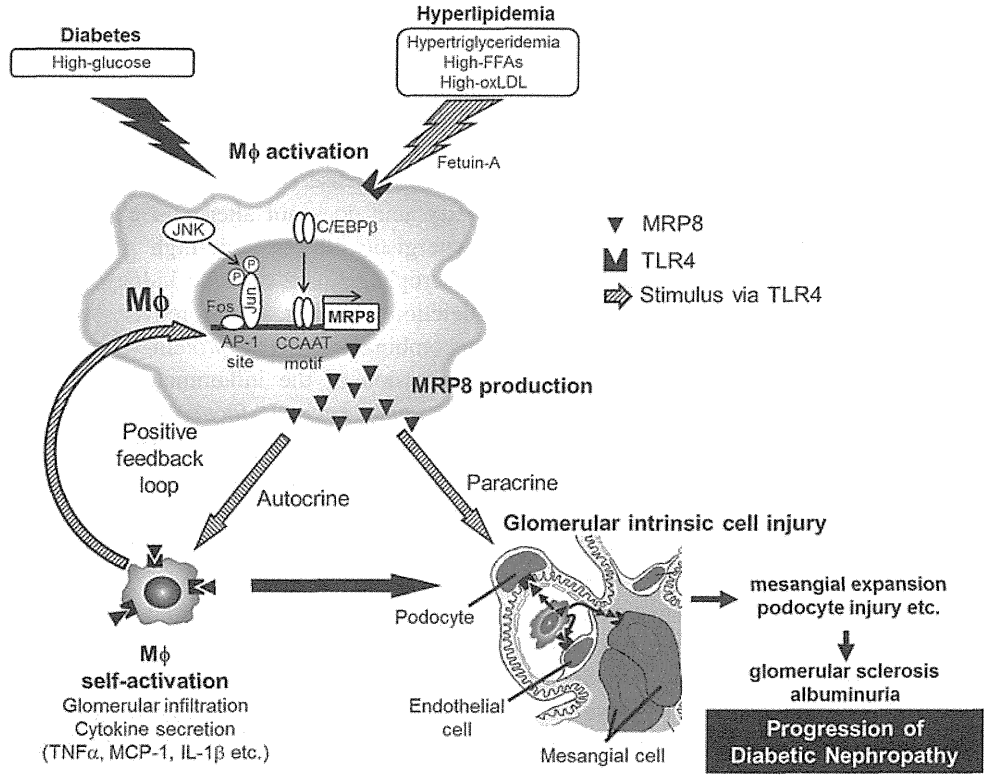

Fig. 5 Proposed mechanism of macrophage-mediated glucolipotoxicity in diabetic nephropathy. Hyperlipidemia (or high free fatty acids) activates circulating macrophages through TLR4-mediated upregulation of MRP8, specifically under hyperglycemic conditions. These synergistic effects upon MRPã8 production in macrophages might be mediated by fetuin A and transcription factors AP-1 and CEBP/β. Macrophage activation is enhanced by a positive feedback, mediated by MRP8/TLR4 interaction in an autocrine fashion. Since glomerular intrinsic cells (such as podocytes, mesangial cells and endothelial cells) reportedly express TLR4, they can be activated through multiple pathways including (1) MRP8 from blood circulation, (2) MRP8 and inflammatory cytokines produced by glomerulus-infiltrating macrophages, and (3) hyperlipidemia. Activation of glomerular cells results in mesangial expansion and podocyte injury, further leading to glomerular sclerosis (fibrosis) and albuminuria

are DN > ORG > MCNS > MGA. Glomerular MRP8 expression is strongly correlated to the extent of proteinuria at 1 year after renal biopsy, whereas tubulointerstitial MRP8 expression is associated with worsening of renal function within a year, suggesting that renal MRP8 expression may become a new biomarker for DN (submitted).